Cisplatin-induced senescence in ovarian cancer cells is mediated by GRP78

WEI LI[1*], WEI WANG[2*], HONG DONG[1], YAN LI[1], LI LI[1], LINFEI HAN[3], ZHIQIANG HAN[1], SHIXUAN WANG[1], DING MA[1] and HUI WANG[1]

[1]Cancer Biology Research Center, Tongji Hospital, Tongji Medical College, Huazhong University of Science and Technology, Wuhan, Hubei 430030; [2]Department of Gynecology and Obstetrics, Nanfang Hospital, Southern Medical University, Guangzhou 510515; [3]Shanghai First Maternity and Infant Health Hospital, Tongji University, Shanghai 200040, P.R. China

Received January 6, 2014; Accepted February 24, 2014

DOI: 10.3892/or.2014.3147

Abstract. Glucose-regulated protein 78 (GRP78), the most abundant and well-characterized glucose-regulated protein, is a major stress-inducible chaperone localized to the endoplasmic reticulum (ER). The purpose of the present study was to investigate the mechanisms of GRP78 involved in the senescence sensitivity of ovarian cancer cells to cisplatin. In the present study, we found that the chemotherapy-sensitive ovarian tumor sections showed strong staining for heterochromatin protein 1-γ (HP1-γ), but weak staining for GRP78. Cisplatin-sensitive A2780 cells with low expression of GRP78 tended to undergo senescence easily when compared with the cisplatin-resistant C13K cells following a dose-gradient cisplatin exposure. Forced overexpression of GRP78 protected the cisplatin-sensitive A2780 cells from cisplatin-induced senescence through P53 and CDC2. Knockdown of GRP78 rescued the senescence sensitivity of cisplatin-resistant C13K cells to cisplatin through P21 and CDC2. Twisting of Ca^{2+} release from ER stores by GRP78 was established to be associated with the sensitivity of cisplatin-induced senescence in ovarian cancer cell lines. In conclusion, GRP78 may have anti-senescence effects on ovarian cancer cells involving multiple mechanisms. Intervention against GRP78 may reduce cisplatin resistance in ovarian cancer.

Correspondence to: Dr Ding Ma or Dr Hui Wang, Cancer Biology Research Center, Tongji Hospital, Tongji Medical College, Huazhong University of Science and Technology, Wuhan, Hubei 430030, P.R. China
E-mail: dma@tjh.tjmu.edu.cn
E-mail: huit71@sohu.com

*Contributed equally

Abbreviations: SAHF, senescence-associated heterochromatic foci; HP1-γ, heterochromatin protein 1-γ; CFSE, carboxyfluorescein succinimidyl ester; siRNA, synthetic small interfering RNA; SA-β-gal, senescence-associated β-galactosidase; GRP78, glucose-regulated protein 78; ER, endoplasmic reticulum; ATM, ataxia telangiectasia mutated; NAC, neoadjuvant chemotherapy

Key words: cell senescence, ovarian cancer, cisplatin, drug-resistance, GRP78, ataxia telangiectasia mutated

Introduction

Cisplatin is a major chemotherapy drug for ovarian cancer; yet, drug-resistance to cisplatin occurs in many ovarian cancer patients, leading to an overall 5-year survival rate of 30-40%. To date, a large number of genes appear to contribute to cisplatin resistance including DNA damage-repair genes, apoptosis-regulating and survival signal-related genes (1-3). The effects of these genes on the cellular response to chemotherapy have been measured by their influence on apoptosis in cancer cells (4,5). Nonetheless, a large number of investigations has verified that cancer cells tend to undergo senescence rather than apoptosis following exposure to DNA-damaging drugs at low-doses similar to those used in clinical applications. Recent data have shown that low, clinically relevant doses of DNA-damaging drugs do not induce apoptosis in epithelial tumor cells but instead lead to a permanent growth arrest associated with cellular senescence (6,7), which was primarily detected by the presence of senescence-associated β-galactosidase (SA-β-gal) and senescence-associated heterochromatin foci (SAHF) such as heterochromatin protein 1-γ (HP1-γ) foci (8,9). Moreover, the presence of SA-β-gal was noted in 41% of specimens from breast cancer patients who received chemotherapy compared with 10% of specimens from patients who underwent surgery without chemotherapy (10), suggesting that chemotherapy induces senescence *in vivo* as well. The latter studies also revealed that cellular senescence contributes to treatment outcome of cancer therapy *in vivo* (11,12). Therefore, senescence plays an important role in the *in vivo* response to chemotherapy. Furthermore, research has shown that cisplatin induces tumor cells to exhibit a senescence-like phenotype and to undergo growth repression (13). However, the mechanisms of action of cisplatin are still unclear.

Glucose-regulated protein 78 (GRP78), the most abundant and well-characterized glucose-regulated protein, is a

major stress-induced chaperone localized in the endoplasmic reticulum (ER) (14). As a calcium-binding protein in the ER, GRP78 serves as a buffer against calcium efflux from the ER that could trigger the mitochondrial apoptotic program (15,16). Moreover, through direct or indirect interactions with specific caspases and other upstream components of the pro-apoptotic pathways initiating from the ER, GRP78 is postulated to regulate the balance between cell survival and apoptosis (17-19). Notably, previous studies found that the cisplatin response also involves ER stress and that GRP78 expression is associated with apoptosis-sensitivity of tumor cells to cisplatin (20-22). However, there is not a clear relationship between GRP78 and cisplatin-induced senescence. It has been shown that GRP78 plays an anti-apoptotic role through altered expression of ataxia telangiectasia mutated (ATM) pathway genes, which were also found to be associated with chemotherapy-induced senescence (23). The relationship between GRP78 and ATM pathway genes in cisplatin-induced senescence has not yet been explored.

In the present study, we first demonstrated that GRP78 expression was significantly lower in chemotherapy-sensitive ovarian tumor sections. We also found that cisplatin-sensitive A2780 cells tended to undergo senescence easily, while cisplatin-resistant C13K cells showed no senescence phenotype after a dose-gradient cisplatin exposure. Inhibition of GRP78 expression rescued the senescence sensitivity of C13K cells to cisplatin. The cisplatin response was found to involve the ATM pathway genes, *P53*, *P21* and *CDC2*, as well as ER calcium homeostasis. Collectively, we demonstrated that GRP78 plays a negative role in cisplatin-induced senescence in ovarian cancer cells, which may contribute to our understanding of the mechanism of the drug-resistance of ovarian cancer cells to cisplatin.

Materials and methods

The present study was reviewed and approved by the Ethics Committee of Tongji Hospital, Tongji Medical College, Huazhong University of Science and Technology (HUST). All experimental protocols were approved by the Institutional Animal Care and Use Committee of HUST, and the study was carried out in strict accordance with the Animal Research: Reporting of In Vivo Experiments (ARRIVE) guidelines.

Cell lines. The cisplatin-sensitive human ovarian cancer cell line A2780 (P53 wild-type) was purchased from the European Collection of Cell Cultures (ECACC). The cisplatin-resistant human ovarian cancer cell line C13K (P53 wild-type) was a gift from Benjamin K. Tsang (Department of Obstetrics and Gynecology and Cellular and Molecular Medicine, University of Ottawa, Canada). A2780 and C13K cells were grown in RPMI-1640 medium with 10% fetal bovine serum (FBS) in a humidified atmosphere of 5% CO_2 at 37˚C. Cisplatin was added for 1 day at the indicated concentrations to cells at 30-40% confluency. The cells were washed twice with phosphate-buffered saline (PBS) and maintained for 6 days in complete medium prior to harvest for analysis. Caffeine was added 2 h before cisplatin exposure. The drug A23187 was added 1 day before exposure to cisplatin or transfection with small-interfering RNA.

Reagents. Rabbit polyclonal antibodies against HP1-γ and GRP78 were purchased from PTG Inc. (Wuhan, China). A rabbit polyclonal antibody against P53 was purchased from Boster Bio-Company (Wuhan, China). A mouse monoclonal antibody against P21 was purchased from Santa Cruz Biotechnology (Santa Cruz, CA, USA). A mouse monoclonal antibody against CDC2 was purchased from BD Company (Franklin Lakes, NJ, USA). A senescence-associated β-galactosidase staining kit and a rabbit polyclonal antibody against p-CDC2 were purchased from Cell Signaling Technology (Beverly, MA, USA). Carboxyfluorescein succinimidyl ester (CFSE) fluorescent dye was purchased from Dojin Co. (Tokyo, Japan). Anti-rabbit IgG labeled with Rhodamine was purchased from Zhongshan Biotech, Co., (Beijing, China). Caffeine was purchased from Alexion (Lausanne, Switzerland). Cisplatin and A23187 were purchased from Sigma Company (Cream Ridge, NJ, USA). RPMI-1640 medium was purchased from Gibco Company (Billings, MT, USA). Fluo3-AM was purchased from Invitrogen Company (Grand Island, NY, USA).

Clinical samples. Tissue specimens were obtained from suspect ovarian tumors during surgery at the Department of Gynecology and Obstetrics, Tongji Hospital, Tongji Medical College, Huazhong University of Science and Technology in China from September 2005 to October 2009. The histological diagnosis of ovarian cancer was confirmed in all cases, and the clinical International Federation of Gynecology and Obstetrics (FIGO) disease stage was used. The 6 patients with stage IV ovarian serous adenocarcinoma tumors were treated with 2-4 cycles of TP (paclitaxel + cisplatin) neoadjuvant chemotherapy (NAC) before surgery. For each patient, a regression coefficient was calculated using CA125 levels measured from the day of NAC (as day 0) until the day their CA125 levels normalized (<35 IU/ml) or the day of standard surgery. A chemotherapy-sensitive sample was defined as having a regression coefficient of ≥-0.039 (3 cases), and a chemotherapy-resistant sample was defined as having a regression coefficient <-0.039 (3 cases). The method used for the calculation of the regression coefficient was performed as described previously (24).

Immunohistochemical analyses. The immunohistochemical analyses were carried out as described previously (25). The negative control slides were processed similarly but with the omission of the primary antibody.

SA-β-galactosidase histochemical staining. Histochemical detection of SA-β-gal was performed with the Senescence SA-β-Galactosidase Staining kit (Cell Signaling) according to the manufacturer's instructions. Briefly, cultured cells were treated with cisplatin as described above. Following treatment, the cells were washed twice with PBS and fixed with a 3.5% paraformaldehyde solution for 15 min at room temperature. The cells were washed every 5 min 3 times in PBS, and the SA-β-gal staining solution (pH 6.0) was added and incubated for 16 h at 37˚C. The percentage of positively stained cells was determined by counting 3 random fields of at least 100 cells each. Images of representative fields were captured under a x20 magnification.

Cell cycle profiling. For cell cycle profiling, the cells were fixed with 75% ice-cold ethanol and stained with 50 μg/ml propidium iodide before fluorescence-activated cell sorting analysis (FACS).

Analysis of cell proliferation by CFSE labeling. CFSE is a green fluorescent dye that is distributed equally among daughter cells with each cell division. For labeling, cells were incubated with 3 μM CFSE in serum-free RPMI-1640 medium for 15 min at 37˚C. Excess dye was removed by two rinses in fresh complete medium. The CFSE-labeled cells were plated in 6-well flat-bottom plates and cultured in fresh complete medium with or without cisplatin for the indicated time. The cells were harvested and examined by flow cytometry. The data were analyzed using the ModFit software (Becton-Dickinson). The cell proliferation model was used to calculate the proliferation index, which is the ratio of the total number of cells analyzed to the calculated number of parent cells required to produce the observed number of cells.

Immunofluorescence. Cells were plated onto 6-well cell culture plates (10,000 cells/well) in which slides were placed previously for immunostaining. Twenty-four hours after plating, the cells were treated with the indicated doses of cisplatin for 1 day; subsequently, cells were washed twice with PBS and maintained for 6 days in fresh medium containing 10% FBS until analysis. Cells were fixed in 75% ethanol for 30 min, permeabilized in 3% Triton X-100 for 5 min, and blocked in 5% normal goat serum in PBS at 37˚C for 1 h. Cells were incubated with the HP1-γ polyclonal antibody (1:50) overnight at 4˚C. After washing, the cells were incubated with goat anti-rabbit immunoglobulin G (IgG)-Rhodamine for 30 min at room temperature. Slides were observed by fluorescence microscopy using a Leica DM4000 B microscope (40x lens objective and 0.75 numerical apertures) with a Qimaging Retiga 1300 camera.

Western blot analysis. Preparation of the protein samples and western blot analyses were carried out as previously described (26). The western blotting antibodies used were the following: GRP78 (1:500), P53 (1:500), P21 (1:500), p-CDC2 (1:500), CDC2 (1:500) and β-actin (1:1,000). After washing in PBS, the membranes were incubated with a secondary antibody at a dilution of 1:1,000. The proteins were visualized using the BCIP/NBT immunoblotting detection system.

Transient siRNA transfection. The annealed synthetic small interfering RNAs (siRNAs) were synthesized by RiboBio Co., Ltd. (Guangzhou, China). The GRP78-specific siRNA (sense sequence, 5'-GAGUGACAGCUGAAGACAAdTdT-3' and antisense sequence, 5'-GCCAGCGCACCTdTd-3') was used to knock down the expression of GRP78. A2780 and C13K cells were plated onto 6-well culture plates at 30% density. After 1 day, the cells were transfected with GRP78-siRNA or control-siRNA with Lipofectamine 2000 (Invitrogen) according to the manufacturer's protocol. Briefly, for each well in a 6-well plate, 5 μl of Lipofectamine 2000 was diluted in 0.25 ml of serum-free RPMI-1640 medium. This mixture was carefully added to a solution containing 50 nmol of siRNA in 0.25 ml of serum-free RPMI-1640 medium. The solution was incubated for 20 min at room temperature and then gently overlaid onto cells at 40-50% confluency in 1.5 ml of serum-free RPMI-1640 medium. After 4-6 h, the cells were cultured with fresh complete medium for 72 h before being exposed to cisplatin.

Animal treatment protocol. All animal procedures were performed in the animal facility in accordance with applicable animal welfare regulations under an approved Institutional Animal Care and Use (IACUC) protocol and study design. Female athymic Balb/c nu/nu mice (5-8 weeks of age; obtained from the Animal Experimental Center of Slaccas, Shanghai, China) were implanted subcutaneously in the right flank with $2x10^6$ A2780 or C13K cells mixed with an equal volume of saline. After 8 days, mice were randomly sorted into 2 groups (n=5 for each group) reflecting different treatment regimens: group 1 received only a saline injection; group 2 was injected twice with cisplatin at a dose of 10 mg/kg in a 3 day interval. The mice were monitored twice a week by inspection and palpitation. Seven days after the first injection, subcutaneous tumors were freshly frozen in Tissue-Tek cryopreservation medium, cryostat sectioned and stored at -20˚C for SA-β-galactosidase staining and immunohistochemical analysis.

Detection of relative Ca^{2+} concentrations. Fluo3-AM exhibits high fluorescence intensity increases on binding Ca^{2+} which is visible with excitation at 488 nm by argon-ion laser sources. Briefly, cells were plated onto glass bottom dishes with a 35-mm diameter. Twelve hours after treatment, the control cells and the cells receiving different types of treatment were washed with D-Hanks for 3 times, incubated with serum-free RPMI-1640 medium containing 4 μM Fluo3-AM and 0.05% Pluronic-F127 for 45 min at 37˚C, protected from light. Then the cells were washed twice with Hanks containing 0.2% BSA, and subsequently washed with Hanks one time for clear up of the residual Fluo3-AM. The cells were observed by using laser confocal microscope with a 488-nm excitation wavelength and 505-530 nm absorption wavelength, 60x objective lens, 1,024x1,024 resolution, at 37˚C. The fluorescent images were collected every 10 sec for 10 times. Ten cells were monitored for each experiment. Three independent experiments were carried out. The mean intensity of Ca^{2+} fluorescence was analyzed with FluoView software.

Statistical analyses. The results are expressed as means ± SE of 3 independent experiments. Statistical significance between groups was determined by ANOVA analysis and defined as $P<0.05$.

Results

GRP78 is related to cisplatin-induced senescence in vivo. To investigate the relationship between GRP78 expression and senescence induced by cisplatin, tumor sections from 6 ovarian cancer patients who had received 2-4 cycles of neoadjuvant chemotherapy were stained for GRP78 and senescence-associated heterochromatin HP1-γ foci. The clinical data showed that 3 of the patients were chemotherapy-resistant, and the other 3 patients were chemotherapy-sensitive (Table I). The chemotherapy-sensitive tumor sections showed strong

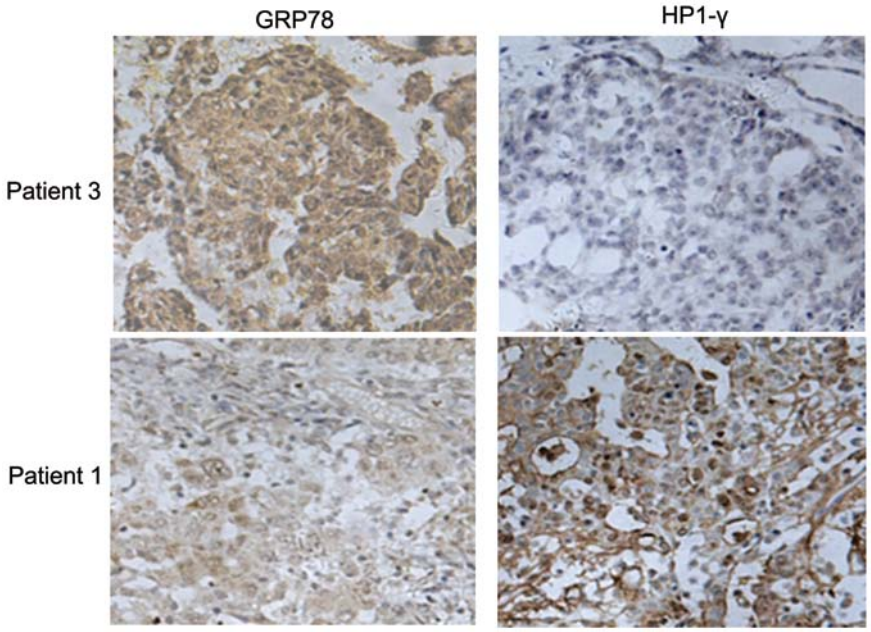

Figure 1. GRP78 and HP1-γ expression. Tumor sections from 6 ovarian cancer patients who had received neoadjuvant chemotherapy were stained using immunochemistry for GRP78 and HP1-γ. (Upper row of images) The chemotherapy-resistant tumor sections from patient 3, who received 2 cycles of neoadjuvant chemotherapy display positive staining for GRP78 and weak staining for HP1-γ. (Lower row of images) The chemotherapy-sensitive tumor sections from patient 1 who received 4 cycles of neoadjuvant chemotherapy show weak staining for GRP78 and intensely positive staining for HP1-γ. GRP78, glucose-regulated protein 78; HP1-γ, heterochromatin protein 1-γ.

Table I. Clinical parameters and outcome of the ovarian cancer patients who underwent neoadjuvant chemotherapy prior to surgery.

Patient no.	FIGO stage	Neoajuvant therapy	GRP78	HP1-γ	Regression coefficient
1	IV	TPx4	+/-	++++	>-0.039
2	IV	TPx2	+	+++	>-0.039
3	IV	TPx2	+++	+/-	<-0.039
4	IV	TPx3	++	+	<-0.039
5	IV	TPx3	++++	+	<-0.039
6	IV	TPx2	+	+++	>-0.039

+/-, Scant/spotty-positive; +, weakly positive; ++ to ++++, intensely positive; GRP78, glucose-regulated protein 78; HP1-γ, heterochromatin protein 1-γ.

staining for HP1-γ, but weak staining for GRP78. We also showed adverse results in the chemotherapy-resistant tumor sections (Fig. 1). These data indicate that GRP78 expression was negatively associated with cisplatin-induced senescence in ovarian cancer.

Exhibition of a senescence phenotype in cisplatin-sensitive A2780 and cisplatin-resistant C13K cells. To study whether cisplatin induces ovarian cancer cells to exhibit a senescence-like phenotype, cisplatin-sensitive A2780 cells and cisplatin-resistant C13K cells were both exposed to a sub-apoptotic dose of cisplatin for 24 h, respectively. The results showed that A2780 cells exhibited a senescence phenotype at day 6 following 3 μg/ml cisplatin treatment. Nearly 90% of the A2780 cells showed an enlarged, flattened morphology, increased cytoplasmic granularity, positive staining of SA-β-gal and massive accumulation of HP1-γ foci (Fig. 2A). The senescent A2780 cells did not further divide as confirmed by the CFSE proliferation index (PI). In the cisplatin-treated A2780 cells, the PI values were 3.1±0.6 and 4.5±0.7 at day 4 and 7 following treatment, respectively, while the PI values were 7.8±1.2 and 15.8±2.4, respectively, in the control cells (Fig. 2B). Furthermore, more than 80% of A2780 cells were arrested at the G2-M phase at day 4 following cisplatin treatment. These effects were mediated by the ATM gene as verified by its abrogation with caffeine pretreatment (5 mmol/l; Fig. 2C).

In contrast to the A2780 cells, C13K cells did not show any senescent phenotype following treatment with various doses of cisplatin ranging from 10 to 20 μg/ml. The staining of SA-β-gal and HP1-γ foci were both negative in the C13K cells treated with a sub-apoptotics dose of cisplatin (20 μg/ml) (Fig. 2A). In addition, C13K cells showed an increased CFSE PI following treatment with 20 μg/ml cisplatin. The PI values of the cisplatin-treated C13K cells were 7.5±1.2 and 14.2±0.5 at day 4 and 7 following treatment, which was similar to the values for the untreated cells (8.9±1.7 and 16.8±3.2, respectively) (Fig. 2B). Less than 30% of C13K cells were arrested at the G2-M phase at day 4 following cisplatin treatment (Fig. 2C).

GRP78 expression in ovarian cancer cells and subcutaneous tumors. To investigate whether GRP78 has an impact on cisplatin-induced senescence, GRP78 expression was detected *in vitro* and *in vivo*. In the A2780 cells, cisplatin treatment resulted in decreased GRP78 protein levels at day 1 and decreased to a minimum at day 2 to 7 (Fig. 3A). *In vivo*, the

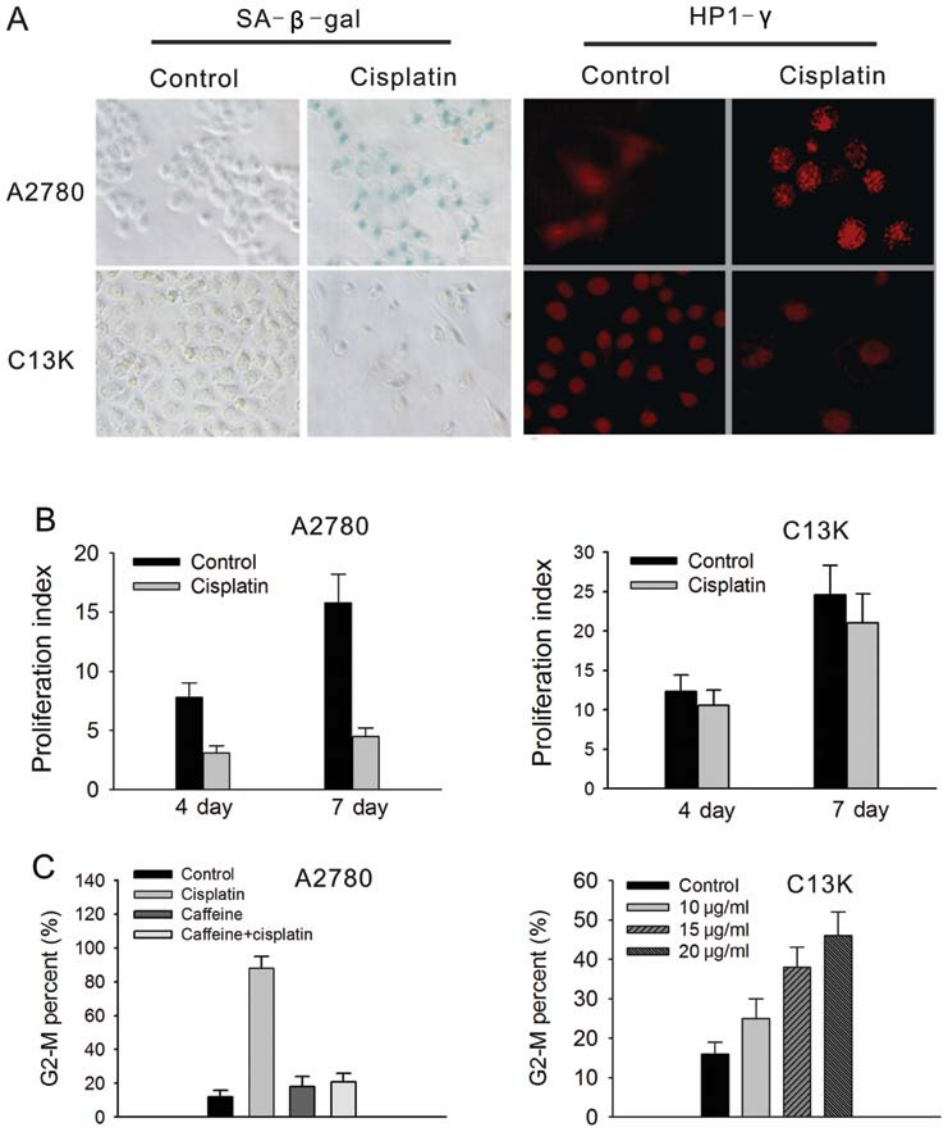

Figure 2. Cisplatin induces a senescence phenotype in cisplatin-sensitive A2780 cells but not in cisplatin-resistant C13K cells. A2780 cells were treated with 3 μg/ml cisplatin. C13K cells were treated with 20 μg/ml cisplatin. (A) A2780 and C13K cells were stained with β-gal at pH 6.0 or with immunofluorescent HP1-γ protein. (B) A2780 and C13K cells were labeled by CFSE to determine the proliferation index at day 4 and 7 following cisplatin treatment. The proliferation index of the untreated cells at day 0 was 1. (C) Four days following treatment with 3 μg/ml cisplatin, or 5 mmol/l caffeine, or a combination of cisplatin and caffeine, A2780 cells were stained with propidium iodide for FACS analysis. Four days following treatment with 10, 15 and 20 μg/ml cisplatin, C13K cells were stained with propidium iodide for FACS analysis. Data are shown as means ± SE of 3 independent experiments. HP1-γ, heterochromatin protein 1-γ; CFSE, carboxyfluorescein succinimidyl ester; FACS, fluorescence-activated cell sorting analysis.

cisplatin-treated subcutaneous tumor sections showed positive staining for SA-β-gal (Fig. 3B; upper row), and GRP78 stainning in the cisplatin-treated tumor sections was significantly weaker than that in the saline-treated tumor sections (Fig. 3B; lower row).

In the C13K cells, compared with the untreated cells, GRP78 protein levels increased at 6 h after exposure to cisplatin and remained elevated at day 7 (Fig. 3A). SA-β-gal staining in both the saline-treated and cisplatin-treated subcutaneous tumor sections was negative (Fig. 3B; upper row), and there was no difference in the GRP78 expression in these two groups (Fig. 3B; lower row).

Overexpression of GRP78 results in A2780 cell resistance to cisplatin-induced senescence, which was accompanied by obvious suppression of P53 expression. A23187 is a mobile ion-carrier that forms stable complexes with divalent cations and has frequently been used to upregulate GRP78 expression. In our experiments, A2780 cells were treated with A23187 at a final concentration of 2.5 mmol/l 1 day before cisplatin treatment. GRP78 protein levels were significantly increased following A23187 exposure, but were significantly decreased following GRP78-siRNA treatment (Fig. 4A). Seven days after 3 μg/ml cisplatin treatment, <20% of the A23187-treated A2780 cells showed positive SA-β-gal staining, whereas cells treated with cisplatin only were almost all positively stained (Fig. 4B). To confirm the specific anti-senescence effect of GRP78, GRP78-siRNA was transfected into the A23187-treated A2780 cells. After 3 days, the treated cells were exposed to 3 μg/ml cisplatin and incubated with complete medium. After 6 days,

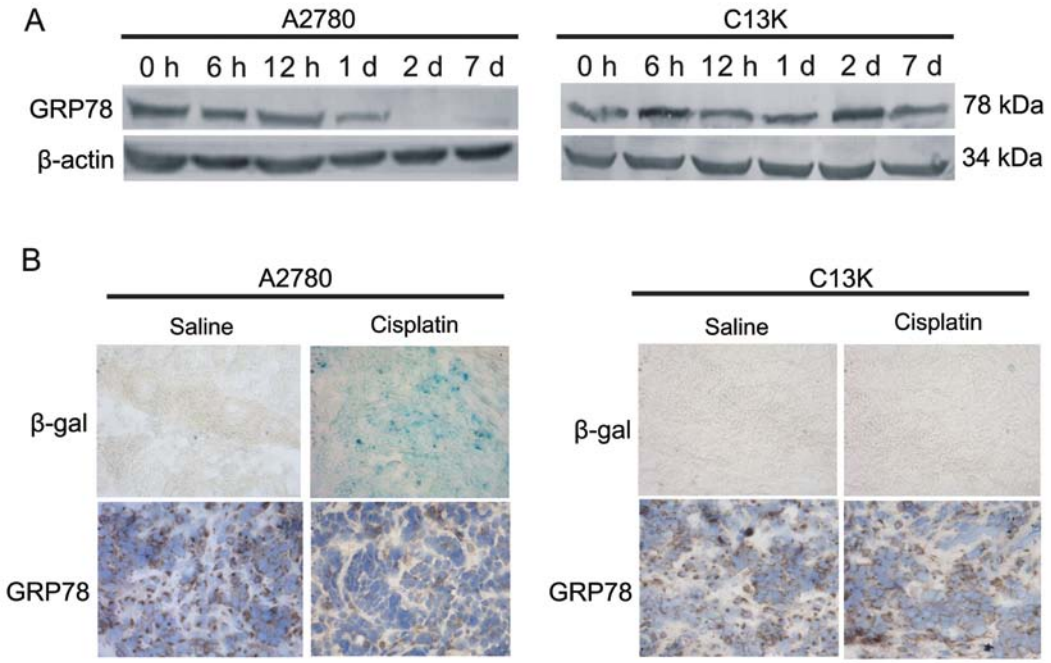

Figure 3. GRP78 expression *in vitro* and *in vivo*. (A) A2780 and C13K cells were treated with 3 or 15 μg/ml cisplatin, and the GRP78 protein level was examined by western blotting at 0, 6 and 12 h; 1, 2 and 7 days. (B) Female athymic Balb/c nu/nu mice were implanted subcutaneously with 2x10^6 A2780 or C13K cells. After 8 days, mice were randomly sorted into 2 groups and received saline injection or cisplatin injection. The subcutaneous tumor sections were stained with SA-β-galactosidase (upper row) and immunochemistry for GRP78 (lower row). The data are representative of results from 3 independent experiments. GRP78, glucose-regulated protein 78.

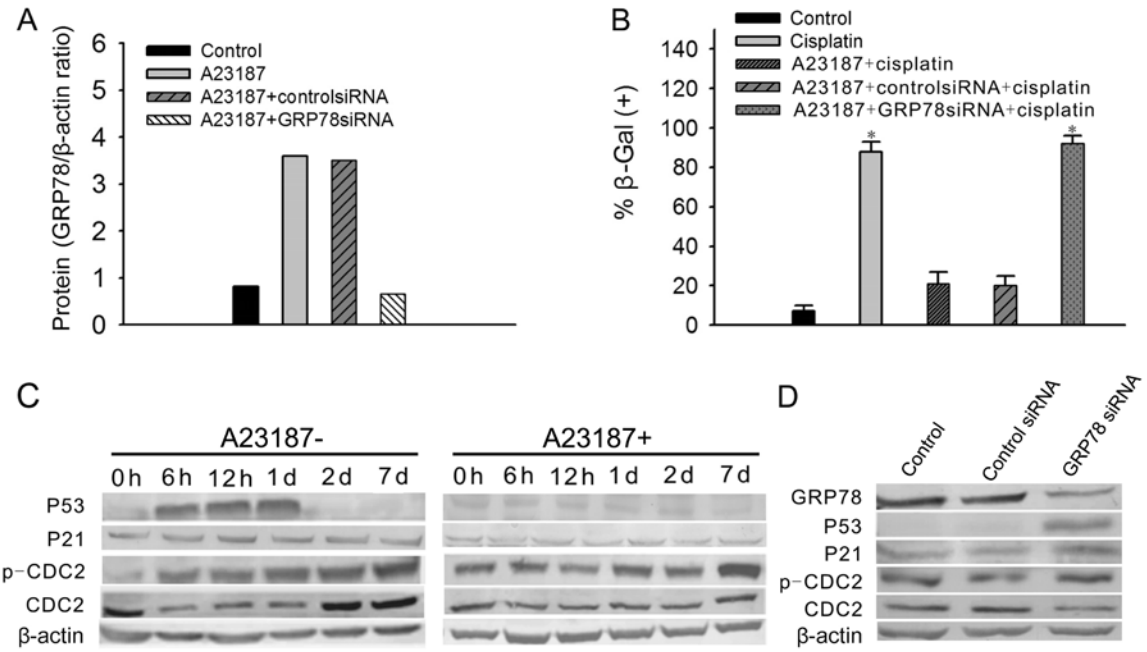

Figure 4. Overexpression of GRP78 results in A2780 cell resistance to cisplatin-induced senescence, requiring suppression of P53 expression. A2780 cells were treated with A23187 at a final concentration of 2.5 mmol/l 1 day before cisplatin treatment. (A) Western blot results of GRP78 detection. A2780 cells were treated with A23187 and transfected with GRP78-siRNA or control-siRNA. (B) Senescence-positive staining rate of cells listed in A following 3 μg/ml cisplatin treatment. (C) Protein levels of ATM pathway genes P53, P21, p-CDC2 and CDC2 were examined by western blot analyses at 0, 6 and 12 h; 1, 2 and 7 days following cisplatin treatment in the presence or absence of A23187 induction. (D) Expression of ATM pathway genes in A2780 cells following GRP78 knockdown. Data are shown as means ± SE of 3 independent experiments. *Significantly different from the control value (P<0.05). GRP78, glucose-regulated protein 78; ATM, ataxia telangiectasia mutated.

the cells exhibited 90% positive SA-β-gal staining (Fig. 4B). These data indicate that overexpression of GRP78 can protect A2780 cells against cisplatin-induced senescence.

To clarify the mechanisms of the senescence-resistant effects of GRP78, levels of the ATM pathway genes in A2780 cells were examined by western blotting at 6 and

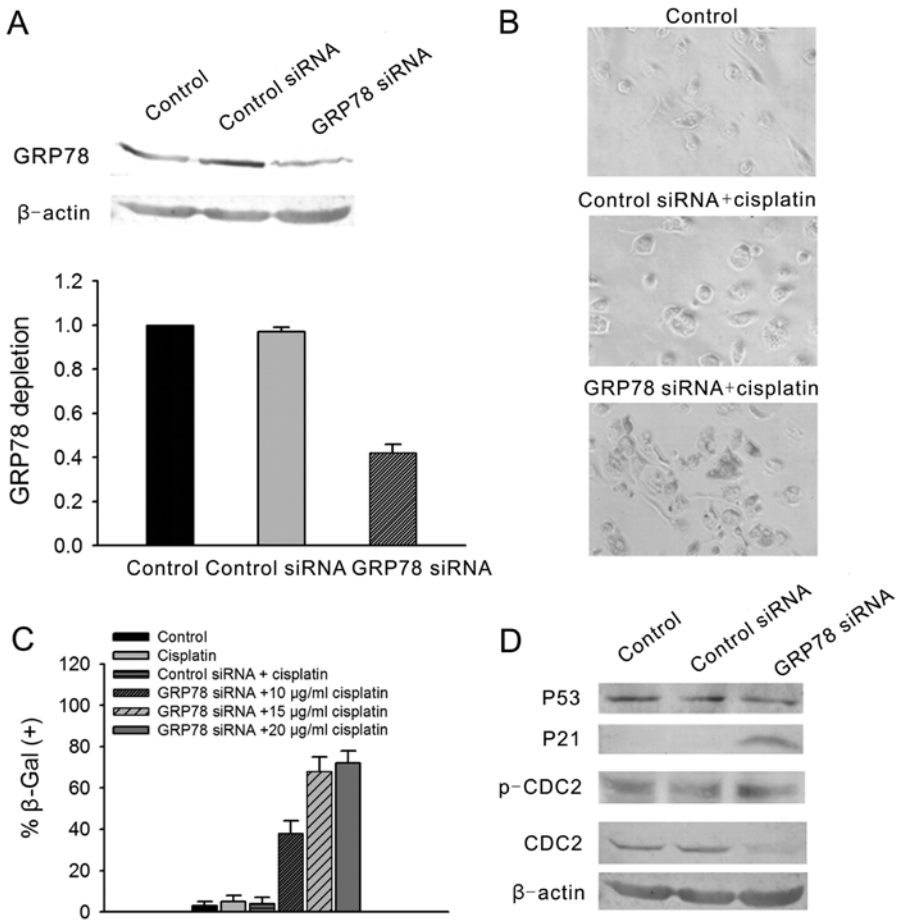

Figure 5. Knockdown of GRP78 rescues the senescence-sensitivity to cisplatin through increase in P21 expression and decrease in CDC2 expression in C13K cells. (A) C13K cells were transfected with GRP78-siRNA or control-siRNA. The cells were collected 3 days after transfection for analysis, and GRP78 expression was examined by western blotting (upper row) and quantified (lower row). (B) Staining for senescence in the cells listed in A following 15 μg/ml cisplatin treatment. (C) The senescence-positive rate of CI3K cells treated with or without cisplatin, and transfected with GRP78-siRNA or control-siRNA. (D) Western blot results for P53, P21, p-CDC2 and CDC2. C13K cells were transfected with GRP78-siRNA or control-siRNA. Data are shown as means ± SE of 3 independent experiments. GRP78, glucose-regulated protein 78.

12 h; 1, 2 and 7 days following cisplatin treatment with or without A23187 exposure. In the non-A23187-treated cells, P53 protein levels were significantly increased from 6 h to 1 day and were diminished at day 2; P21 levels were slightly decreased following exposure to cisplatin. CDC2 levels were significantly decreased at day 1 following exposure to cisplatin but were significantly increased from day 2 to 7. p-CDC2 levels were significantly increased from 6 h to 7 days. However, in the A23187-treated cells, there were no changes in the protein levels of P53 and CDC2 following cisplatin exposure. The changes in the protein levels of p-CDC2 and P21 were consistent with those in the non-A23187-treated A2780 cells (Fig. 4C).

Moreover, the ATM pathway gene protein levels were examined by western blotting after knockdown of GRP78. The results showed that GRP78 protein levels were significantly decreased after GRP78-siRNA transfection in the A2780 cells. Accompanied by knockdown of GRP78, P53 levels were significantly increased and CDC2 levels were significantly decreased. There were no changes in the protein levels of P21 and p-CDC2 (Fig. 4D). This suggests that P53 and CDC2 are involved in cisplatin-induced senescence of A2780 cells.

Knockdown of GRP78 rescues the senescence sensitivity of C13K cells to cisplatin through an increase in P21 expression and a decrease in CDC2 expression. To investigate whether GRP78 rescues the senescence sensitivity in C13K cells to cisplatin, GRP78 expression was knocked down by GRP78-siRNA (Fig. 5A). Then, the senescence sensitivity of C13K cells to cisplatin was detected by β-gal staining. After a 1-day incubation with 10, 15 or 20 μg /ml cisplatin, the C13K cells transfected with GRP78-siRNA exhibited a significant senescence phenotype at day 7 following exposure to cisplatin (Fig. 5B and C).

At the same time, we detected the expression of ATM pathway genes in the C13K cells. The results showed that P21 levels were significantly increased and CDC2 levels were significantly decreased following GRP78-siRNA transfection. In contrast, no changes in P53 and p-CDC2 levels were noted (Fig. 5D).

Twisting of Ca^{2+} release from ER stores by GRP78 is associated with the sensitivity of cisplatin-induced senescence in ovarian cancer cell lines. GRP78 is a major ER chaperone with Ca^{2+}-binding property, which can preserve ER calcium

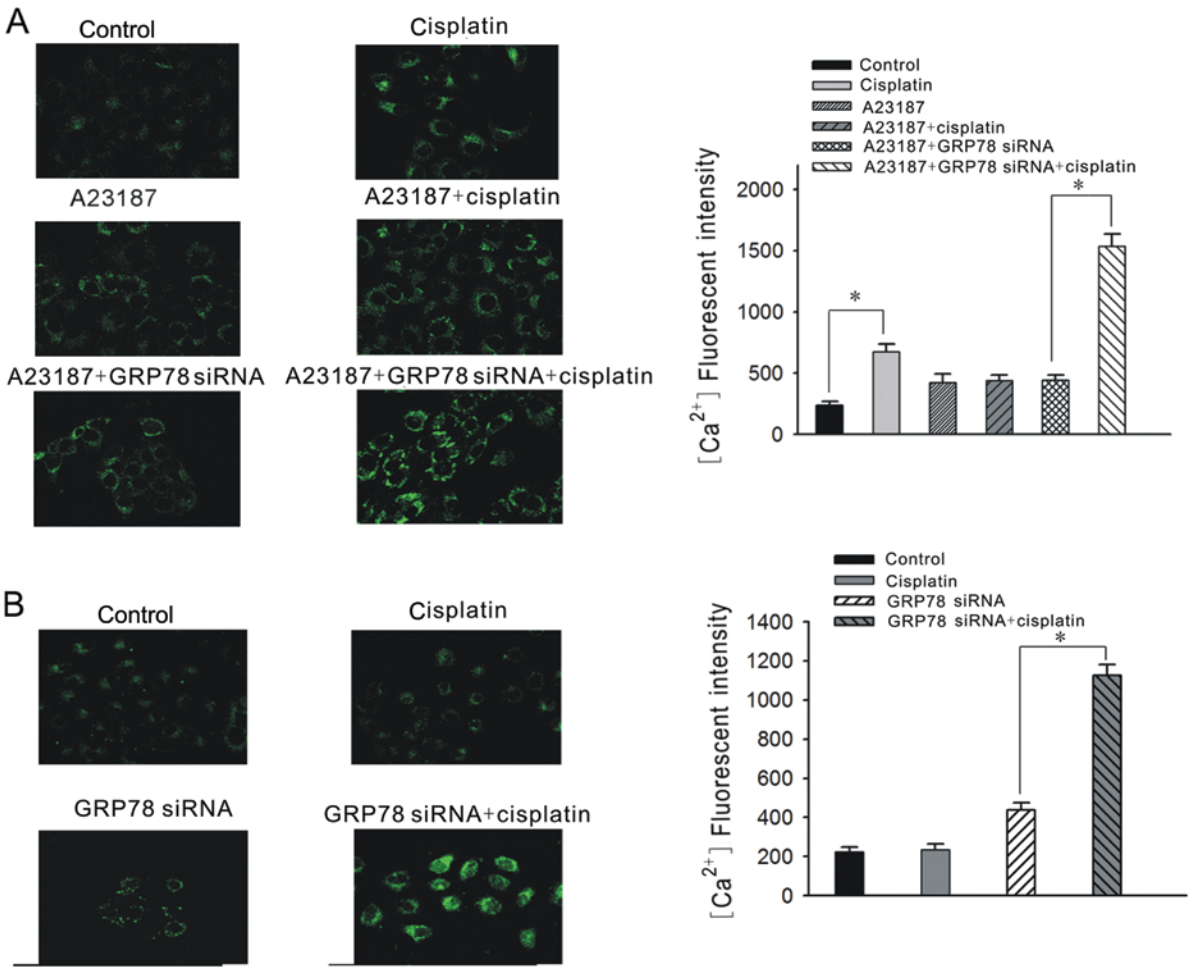

Figure 6. Relative cytoplasmic Ca^{2+} concentration in A2780 and C13K cells. The Ca^{2+} fluorescence intensities are presented as the means ± standard error (n=3). (A) A2780 cells were treated with A23187 at a final concentration of 2.5 mmol/l 1 day before 3 μg/ml cisplatin treatment or GRP78-siRNA transfection. A2780 cells were treated with 3 μg/ml cisplatin 3 days following GRP78-siRNA transfection. Ca^{2+} fluorescence of cells was detected following staining with Fluo3-AM 12 h after cisplatin treatment (left) and analyzed by FluoView software, respectively (right). (B) C13K cells were treated with 3 μg/ml cisplatin 3 days after GRP78-siRNA transfection. Ca^{2+} fluorescence of cells was determined following staining with Fluo3-AM 12 h after cisplatin treatment (left) and analyzed by FluoView software, respectively (right). Data are shown as means ± SE of 3 independent experiments. *Significantly different ($P<0.05$). GRP78, glucose-regulated protein 78.

homeostasis. Therefore, we examined changes in the relative cellular Ca^{2+} concentration to ascertain whether it is relevant to the sensitivity of cisplatin-induced senescence.

In the A2780 cells, the cellular Ca^{2+} concentration was elevated ~3-fold following a 12-h exposure to 3 μg/ml cisplatin. Nonetheless, with a previous A23187 induction for 24 h, the cellular Ca^{2+} concentration was not evidently increased at 12 h following cisplatin treatment. When GRP78 overexpression was suppressed by GRP78-siRNA, the cellular Ca^{2+} concentration was significantly elevated again at 12 h following cisplatin treatment (Fig. 6A).

In the C13K cells, the cellular Ca^{2+} concentration was not obviously elevated following a 12-h exposure to 20 μg/ml cisplatin. Nonetheless, the cellular concentration increased nearly 3-fold at 12 h following 20 μg/ml cisplatin treatment with previous GRP78 suppression by GRP78-siRNA (Fig. 6B). It appears that the capacity of Ca^{2+} release from ER stores may be associated with the sensitivity of cisplatin-induced senescence. GRP78 may influence the sensitivity through twisting the Ca^{2+} release from ER stores.

Discussion

In the present study, we showed that GRP78 expression is negatively associated with cisplatin-induced senescence *in vitro* and *in vivo*. Cisplatin-sensitive A2780 cells exhibited a senescence phenotype, while cisplatin-resistant C13K cells showed no senescence phenotype following a dose-gradient cisplatin exposure. Knockdown of GRP78 expression rescued the senescence sensitivity of C13K cells to cisplatin. The ATM pathway genes such as *P53*, *P21* and *CDC2*, and ER calcium homeostasis were involved in the cisplatin-induced senescence.

GRP78 is a major stress-induced chaperone localized to the endoplasmic reticulum. GRP78 has been examined in human breast carcinomas, and its overexpression has been observed in the majority of the more aggressive estrogen receptor-negative tumors (27). Preliminary analysis of GRP78 in a series of primary and recurrent breast, prostate and lung cancer samples suggest a correlation between GRP78 overexpression and tumor recurrence and drug resistance (28). Moreover, GRP78 has been gradually used as a potent target for diagnosis and

therapy of different types of cancers (29). Synthetic chimeric peptides targeted against GRP78 were found to suppress tumor growth in xenograft and isogenic mouse models of breast and prostate cancer (30). Research has also indicated that GRP78 is associated with the apoptosis of tumor cell lines (31).

In the present study, we firstly investigated the relationship between GRP78 expression and chemotherapy-induced senescence in ovarian cancer patients. The data showed that GRP78 expression was significantly higher in the chemotherapy-resistant tumor samples with weak HP1-γ staining than that of the chemotherapy-sensitive samples with obvious HP1-γ staining. It was suggested that GRP78 may mediate chemotherapy-induced senescence and play a crucial role in the drug resistance in ovarian cancer.

Next, we observed the senescence phenotype in ovarian cancer cells. The results showed that cisplatin-sensitive A2780 cells exhibited an obvious senescent phenotype following cisplatin treatment, and most of the A2780 cells were arrested at the G2/M phase. Accompanied by senescence, GRP78 levels gradually decreased following cisplatin treatment. Conversely, cisplatin-resistant C13K cells did not present a senescent phenotype after a dose-gradient cisplatin exposure, while GRP78 levels increased. Moreover, we also obtained a similar result in the subcutaneous tumor samples. Therefore, GRP78 expression is related with the cisplatin-induced senescence in ovarian cancer cells.

ATM pathway genes are closely associated with senescence. Therefore, we investigated the relationship between GRP78 and the ATM pathway genes during cisplatin-induced senescence in ovarian cancer cells. In the A2780 cells, GRP78 overexpression protected the cells against cisplatin-induced senescence, which was mainly through the suppression of P53 expression. In addition, knockdown of GRP78 resulted in noticeably increased P53 levels. Studies have shown that wild-type p53 limits cellular proliferation by inducing senescence, depending on the expression level or cellular context (32,33). An increase in p53 transcriptional activity is a molecular signature for cellular senescence. It could be postulated that P21-independent P53 expression is a requirement for cisplatin-induced senescence in A2780 cells.

In the C13K cells, knockdown of GRP78 resulted in significantly enhanced senescence sensitivity to cisplatin, which occurred mainly through increased P21 levels and decreased CDC2 levels. Nonetheless, there was no change in P53 levels. P21, a transcriptional target of P53, can inhibit Cdk activity (34). It has been clearly established that P21 is highly related to senescence, and induces senescence in the P53-independent pathway (35,36). CDC2 is the most important gene controlling the cell cycle transition from the G2 to M phase. Decreased CDC2 expression and increased expression of its non-active (15-Tyr)-phosphorylated CDC2 often occurs at G2/M phase arrest and senescence (37). It appears that GRP78-suppression induced senescence was P53-independent in the cisplatin-resistant C13K cells.

Research has revealed that calcium is related to apoptosis (38). Nonetheless, the relationship between calcium and senescence has not been explored. As GRP78 is a major ER protein controlling the calcium efflux from the ER to the cytoplasm, we investigated the association between the change in calcium concentration in the cytoplasm and cisplatin-induced senescence. In the A2780 cells, GRP78 overexpression induced by A23187 obstructed calcium efflux from the ER to the cytoplasm and protected against cisplatin-induced senescence. Conversely, knockdown of GRP78 retrieved the calcium efflux from the ER to the cytoplasm and recovered the senescence sensitivity to cisplatin; whereas, there was no calcium efflux from the ER after cisplatin treatment in the C13K cells, which were senescence-resistant, and suppression of GRP78 expression led to the calcium efflux from the ER to the cytoplasm after cisplatin-treatment and recovered the senescence-sensitivity. According to the results, calcium efflux from the ER to the cytoplasm, which is controlled by GRP78, is essential for cisplatin-induced senescence.

In conclusion, our data showed that GRP78 plays an anti-senescence role in ovarian cancer cells through changes in the expression of ATM pathway genes and calcium efflux from the ER to the cytoplasm. Therefore, targeting against GRP78 may reduce the drug-resistance of ovarian cancer to cisplatin.

Acknowledgements

This study was supported by grants from the National Basic Research Program of China 973 Program, and the National Natural Science Foundation of China (nos. 2013CB911304, 81072132, 81001152, 81101963, 81172466 and 30872751).

References

1. Selvakumaran M, Pisarcik DA, Bao R, Yeung AT and Hamilton TC: Enhanced cisplatin cytotoxicity by disturbing the nucleotide excision repair pathway in ovarian cancer cell lines. Cancer Res 63: 11-16, 2003.
2. Yang X, Xing H, Gao Q, Chen G, Lu Y, Wang S and Ma D: Regulation of HtrA2/Omi by X-linked inhibitor of apoptosis protein in chemoresistance in human ovarian cancer cells. Gynecol Oncol 97: 413-421, 2005.
3. Lee S, Choi EJ, Jin C and Kim DH: Activation of PI3K/Akt pathway by PTEN reduction and *PIK3CA* mRNA amplification contributes to cisplatin resistance in an ovarian cancer cell line. Gynecol Oncol 97: 26-34, 2005.
4. Gifford G, Paul J, Vasey PA, Kaye SB and Brown R: The acquisition of *hMLH1* methylation in plasma DNA after chemotherapy predicts poor survival for ovarian cancer patients. Clin Cancer Res 10: 4420-4426, 2004.
5. Williams J, Lucas PC, Griffith KA, *et al*: Expression of Bcl-xL in ovarian carcinoma is associated with chemoresistance and recurrent disease. Gynecol Oncol 96: 287-295, 2005.
6. Roninson IB: Tumor cell senescence in cancer treatment. Cancer Res 63: 2705-2715, 2003.
7. Elmore LW, Xu Di, Dumur C, Holt SE and Gewirtz DA: Evasion of a single-step, chemotherapy-induced senescence in breast cancer cells: implications for treatment response. Clin Cancer Res 11: 2637-2643, 2005.
8. Lee BY, Han JA, Im JS, *et al*: Senescence-associated β-galactosidase is lysosomal β-galactosidase. Aging Cell 5: 187-195, 2006.
9. Bartkova J, Rezaei N, Liontos M, *et al*: Oncogene-induced senescence is part of the tumorigenesis barrier imposed by DNA damage checkpoints. Nature 444: 633-637, 2006.
10. te Poele RH, Okorokov AL, Jardine L, Cummings J and Joel SP: DNA damage is able to induce senescence in tumor cells in vitro and in vivo. Cancer Res 62: 1876-1883, 2002.
11. Schmitt CA, Fridman JS, Yang M, *et al*: A senescence program controlled by p53 and $p16^{INK4a}$ contributes to the outcome of cancer therapy. Cell 109: 335-346, 2002.
12. Roninson IB: Tumour senescence as a determinant of drug response in vivo. Drug Resist Updat 5: 204-208, 2002.
13. Fang K, Chiu CC, Li CH, Chang YT and Hwang HT: Cisplatin-induced senescence and growth inhibition in human non-small cell lung cancer cells with ectopic transfer of $p16^{INK4a}$. Oncol Res 16: 479-488, 2007.

14. Lee AS: The glucose-regulated proteins: stress induction and clinical applications. Trends Biochem Sci 26: 504-510, 2001.
15. Ranganathan AC, Zhang L, Adam AP and Aguirre-Ghiso JA: Functional coupling of p38-induced up-regulation of BiP and activation of RNA-dependent protein kinase-like endoplasmic reticulum kinase to drug resistance of dormant carcinoma cells. Cancer Res 66: 1702-1711, 2006.
16. Fu Y, Li J and Lee AS: GRP78/BiP inhibits endoplasmic reticulum BIK and protects human breast cancer cells against estrogen-starvation induced apoptosis. Cancer Res 67: 3734-3740, 2007.
17. Reddy RK, Mao C, Baumeister P, Austin RC, Kaufman RJ and Lee AS: Endoplasmic reticulum chaperone protein GRP78 protects cells from apoptosis induced by topoisomerase inhibitors: role of ATP binding site in suppression of caspase-7 activation. J Biol Chem 278: 20915-20924, 2003.
18. Ermakova SP, Kang BS, Choi BY, *et al*: (-)-Epigallocatechin gallate overcomes resistance to etoposide-induced cell death by targeting the molecular chaperone glucose-regulated protein 78. Cancer Res 66: 9260-9269, 2006.
19. Davidson DJ, Haskell C, Majest S, *et al*: Kringle 5 of human plasminogen induces apoptosis of endothelial and tumour cells through surface-expressed glucose-regulated protein 78. Cancer Res 65: 4663-4672, 2005.
20. Mandic A, Hansson J, Linder S and Shoshan MC: Cisplatin induces endoplasmic reticulum stress and nucleus-independent apoptotic signaling. J Biol Chem 278: 9100-9106, 2003.
21. Lee H K, Xiang CL, Cazacu S, *et al*: GRP78 is overexpressed in glioblastomas and regulates glioma cell growth and apoptosis. Neuro Oncol 10: 236-243, 2008.
22. Jiang CC, Mao ZG, Avery-Kiejda K, Wade M, Hersey P and Zhang XD: Glucose-regulated protein 78 antagonizes cisplatin and adriamycin in human melanoma cells. Carcinogenesis 30: 197-204, 2009.
23. Zu K, Bihani T, Lin A, Park YM, Mori K and Ip C: Enhanced selenium effect on growth arrest by BiP/GRP78 knockdown in p53-null human prostate cancer cells. Oncogene 25: 546-554, 2006.
24. Tate S, Hirai Y, Takeshima N and Hasumi K: CA125 regression during neoadjuvant chemotherapy as an independent prognostic factor for survival in patients with advanced ovarian serous adenocarcinoma. Gynecol Oncol 96: 143-149, 2005.
25. Wang W, Wang S, Song X, *et al*: The relationship between c-FLIP expression and human papillomavirus *E2* gene disruption in cervical carcinogenesis. Gynecol Oncol 105: 571-577, 2007.
26. Hawkins LK, Johnson L, Bauzon M, *et al*: Gene delivery from the E3 region of replicating human adenovirus: evaluation of the 6.7 K/gp19 K region. Gene Ther 8: 1123-1131, 2001.
27. Fernandez PM, Tabbara SO, Jacobs LK, *et al*: Overexpression of the glucose-regulated stress gene GRP78 in malignant but not benign human breast lesions. Breast Cancer Res Treat 59: 15-26, 2000.
28. Koomägi R, Mattern J and Volm M: Glucose-related protein (GRP78) and its relationship to the drug-resistance proteins P170, GST-pi, LRP56 and angiogenesis in non-small cell lung carcinomas. Anticancer Res 19: 4333-4336, 1999.
29. Taylor DD, Gercel-Taylor C and Parker LP: Patient-derived tumor-reactive antibodies as diagnostic markers for ovarian cancer. Gynecol Oncol 115: 112-120, 2009.
30. Arap MA, Lahdenranta J, Mintz PJ, *et al*: Cell surface expression of the stress response chaperone GRP78 enables tumor targeting by circulating ligands. Cancer Cell 6: 275-284, 2004.
31. Zhou H, Zhang Y, Fu Y, Chan L and Lee AS: Novel mechanism of anti-apoptotic function of 78-kDa glucose-regulated protein (GRP78): endocrine resistance factor in breast cancer, through release of B-cell lymphoma 2 (BCL-2) from BCL-2-interacting killer (BIK). J Biol Chem 286: 25687-25696, 2011.
32. Petroulakis E, Parsyan A, Dowling RJ, *et al*: p53-dependent translational control of senescence and transformation via 4E-BPs. Cancer Cell 16: 439-446, 2009.
33. Gannon HS, Donehower LA, Lyle S and Jones SN: Mdm2-p53 signaling regulates epidermal stem cell senescence and premature aging phenotypes in mouse skin. Dev Biol 353: 1-9, 2011.
34. Vaziri H, West MD, Allsopp RC, *et al*: ATM-dependent telomere loss in aging human diploid fibroblasts and DNA damage lead to the post-translational activation of p53 protein involving poly(ADP-ribose) polymerase. EMBO J 16: 6018-6033, 1997.
35. Abbas T and Dutta A: p21 in cancer: intricate networks and multiple activities. Nat Rev Cancer 9: 400-414, 2009.
36. Shen H and Maki CG: Persistent p21 expression after Nutlin-3a removal is associated with senescence-like arrest in 4N cells. J Biol Chem 285: 23105-23114, 2010.
37. Roberson RS, Kussick SJ, Vallieres E, Chen SY and Wu DY: Escape from therapy-induced accelerated cellular senescence in p53-null lung cancer cells and in human lung cancers. Cancer Res 65: 2795-2803, 2005.
38. Giorgi C, Ito K, Lin HK, *et al*: PML regulates apoptosis at endoplasmic reticulum by modulating calcium release. Science 330: 1247-1251, 2010.